

# High-overtone Bulk-Acoustic Resonator gravimetric sensitivity: towards wideband acoustic spectroscopy

D. Rabus,<sup>a)</sup> J.M. Friedt,<sup>a)</sup> S. Ballandras,<sup>b)</sup> T. Baron,<sup>c)</sup> É. Lebrasseur,<sup>c)</sup> and É. Carry<sup>c)</sup>

(Dated: 10 August 2015)

In the context of direct detection sensors with compact dimensions, we investigate the gravimetric sensitivity of High-overtone Bulk Acoustic Resonators, through modeling of their acoustic characteristics and experiment. The high frequency characterizing such devices is expected to induce a significant effect when the acoustic field boundary conditions are modified by a thin adlayer. Furthermore, the multimode spectral characteristics is considered for wideband acoustic spectroscopy of the adlayer, once the gravimetric sensitivity dependence of the various overtones is established. Finally, means of improving the gravimetric sensitivity by confining the acoustic field in a low acoustic-impedance layer is theoretically established.

PACS numbers: 43.40

Keywords: HBAR, Resonator, Gravimetric sensitivity

## I. INTRODUCTION

Direct detection sensors<sup>1</sup> aim at continuous, real time monitoring of the presence and concentration of chemical compounds without the need of a preliminary sample preparation step. Amongst the various direct detection strategies including electrochemical methods<sup>2,3</sup>, optical methods (surface plasmon resonance, integrated optics or spectroscopies<sup>4,5</sup>), the use of acoustic waves to probe medium property variations is considered in contexts in which other strategies are not suitable either due to the fragile optical setups or because the compound being investigated is not electrochemically active. The two broad strategies of acoustic transducers aim at observing either boundary condition variations due to the absorption of a thin film on a substrate in which the acoustic wave is confined (the so-called Quartz Crystal Microbalance – QCM<sup>6,7</sup>), or acoustic velocity variations as the boundary conditions are varied by chemical absorption on the surface of the transducer guiding the propagation of a wave confined to the piezoelectric transducer surface (the so-called Surface Acoustic Wave – SAW). Various wave polarization conditions meet the surface confinement requirements but only pure shear waves and waves exhibiting acoustic velocities slower than those of the surrounding medium will prevent radiation losses as the sensor is loaded by a liquid: the former approach is implemented in the Love mode transducer concept<sup>8,9</sup> and the latter in the Lamb wave transducer. All these strategies have been thoroughly investigated in the context of direct detection (bio)sensors. The evolution from the QCM to

the SAW strategy has been motivated by the consideration that rising acoustic frequencies lowers the acoustic wavelength and hence magnifies the effect of a chemical species absorption to form a layer of a given thickness: the gravimetric sensitivity quantifies this notion. Rising QCM frequency classically means lowering the substrate thickness and hence making the transducer more fragile. An alternative consideration here is to use a thin piezoelectric film over a thick substrate selected for its low acoustic losses to both provide high acoustic frequency modes and yet a rugged transducer.

The work presented here focuses on the study of the gravimetric sensitivity by modeling the acoustic transducer electrical response with a one dimensional model. The dependency of the gravimetric sensitivity on the working frequency is demonstrated. The influence of the adsorbed thickness of the added layer and its acoustic properties on the gravimetric sensitivity is also presented. A discussion is proposed on the gravimetric sensitivity definition which depends on the considered initial condition. A maximum of sensitivity is also obtained for a particular thickness in function of acoustic wavelength. The theoretical results are compared with experimental results obtained by considering copper thin film deposition in dry and wet environments. Finally a way to improve the gravimetric sensitivity is proposed using an appropriate added layer on the sensing surface of the transducer.

## II. ACOUSTIC WAVE TRANSDUCERS

The High-overtone Bulk-Acoustic Resonator (HBAR) concept has evolved from the bulk-acoustic resonator (QCM) strategy by identifying a technological limitation to how thin a piezoelectric film could be made when aiming at rising operating frequencies  $f_0$ <sup>10,11</sup>. Since a QCM confines half a wavelength  $\lambda$  in the substrate thickness  $t$ , the resonator frequency is related to the acoustic velocity  $v$  by  $f_0 = c/\lambda = v/(2t)$ : reaching low  $t$  values has been investigated in the free membrane strategy of the Film Bulk Acoustic Resonator (FBAR)<sup>12,13</sup>. The HBAR pre-

<sup>a)</sup>FEMTO-ST, UMR CNRS-UFC-ENSMM-UTBM 6174, ENSMM, 26 Chemin de l'Épitaphe, 25030 Besançon Cedex, France; SENSEOR, Temis Innovation, 18 rue Alain Savary, 25000 Besançon, France

<sup>b)</sup>Frec|n|sys, Temis Innovation, 18 rue Alain Savary, 25000 Besançon, France

<sup>c)</sup>FEMTO-ST, UMR CNRS-UFC-ENSMM-UTBM 6174, ENSMM, 26 Chemin de l'Épitaphe, 25030 Besançon Cedex, France

vents the fragile piezoelectric membrane from collapsing by being supported on a low acoustic loss substrate.

This work focuses on the determination of gravimetric sensitivity (Eq. 1) of HBAR to assess the possibility of using such a transducer for direct detection, and various sensing strategies introduced by the unique spectral properties of the device. Assuming a linear relation between an adsorbed mass  $\Delta m$  and the transducer resonance frequency shift  $\Delta f$ , the gravimetric sensitivity  $S$  is defined as the relative frequency shift  $\frac{\Delta f}{f_0}$  of the resonance when loading the sensing area  $A$

$$S = \frac{\Delta f}{f_0} \times \frac{A}{\Delta m} = \frac{\Delta f}{f_0} \times \frac{1}{\rho \times \Delta t} \quad (1)$$

since  $\Delta m = A\rho\Delta t$  with  $\rho$  the adsorbed layer density and  $\Delta t$  its thickness.

Eq. 1 is used throughout this work for computing  $S$  out of the modeled acoustic transducer frequency variation due to layers with various properties being added over the transducer surface. **However, another practical quantity relating directly frequency shift and adsorbed mass is the mass-sensitivity constant  $C = \frac{\Delta m}{A \cdot \Delta f}$  in  $\text{ng} \cdot \text{cm}^{-2} \cdot \text{Hz}^{-1}$ : the relationship between these two quantities is  $C = \frac{10^9}{S \cdot f_0}$ .**

The perturbative approach of Sauerbrey<sup>14</sup> predicts (Eq. 2) a gravimetric sensitivity only dependent on the transducer thickness  $t_p$  and the density of the piezoelectric material  $\rho_p$ , assuming the adsorbed layer is characterized by  $\rho = \rho_p$ . Hence, a perturbative model hints at a lack of improvement of the gravimetric sensitivity when using high overtone devices which are expected to always exhibit the fundamental mode gravimetric sensitivity.

$$S = \frac{1}{\rho_p \cdot t_p} \quad (2)$$

which results from considering, in a perturbative approach, that  $\frac{\Delta f}{f} = \frac{\Delta \lambda}{\lambda}$  and that the wavelength  $\lambda_n$  of the  $n$ th overtone is related to the substrate thickness by  $t_p = \frac{n\lambda_n}{2}$ , so that Eq. 1 can be written for each overtone of the QCM as

$$S = \frac{\Delta f_n}{f_n} \times \frac{2}{\rho_p n \Delta \lambda_n} = \frac{\Delta \lambda_n}{\lambda_n} \times \frac{2}{\rho_p n \Delta \lambda_n} = \frac{2}{\rho_p \times \lambda_1} \quad (3)$$

with  $\lambda_1 = n \cdot \lambda_n = t_p/2$  the wavelength of the fundamental mode.

Numerical modeling will however be considered to finely analyze the gravimetric sensitivity of HBAR overtones beyond these perturbative assumptions, if only because the HBAR is a complex structure yielding more complex behaviours than this expected constant gravimetric sensitivity with overtone number. **Once the sensitivity is established, the detection limit for a resonator operating at frequency  $f_0$  and exhibiting a quality factor  $Q$  is given by the phase to frequency slope  $\frac{d\varphi}{df} = \frac{2Q}{f_0}$ . From the sensitivity definition, knowing the smallest detectable phase shift  $d\varphi_{min}$  as given in our case in<sup>15</sup>, then the smallest relative detectable frequency shift is**

**$\frac{df_{min}}{f_0} = \frac{d\varphi_{min}}{2Q}$  and  $S = \frac{df}{f_0} \times \frac{A}{dm} \Leftrightarrow \frac{dm}{A} = \frac{1}{S} \times \frac{df}{f_0} \Rightarrow \frac{dm_{min}}{A} = \frac{d\varphi_{min}}{2Q} \times \frac{1}{S}$ . As an example of a numerical application, considering a quality factor of  $Q = 10000$  and a minimum detectable phase variation<sup>15</sup> of  $d\varphi_{min} = 25 \text{ m}^\circ$  and  $S = 150 \text{ cm}^2/\text{g}$ , then  $\frac{dm_{min}}{A} \simeq 4 \text{ ng}/\text{cm}^2$ .**

A HBAR device is a composite resonator including two layers: a thin piezoelectric layer (as a thin QCM) to generate the acoustic wave, and a low acoustic loss substrate used as a cavity to confine the resonances while supporting the thin piezoelectric film. This coupled resonator structure induces a complex admittance spectrum (Fig. 1) with a series of narrow resonances whose amplitudes are modulated throughout the spectrum.

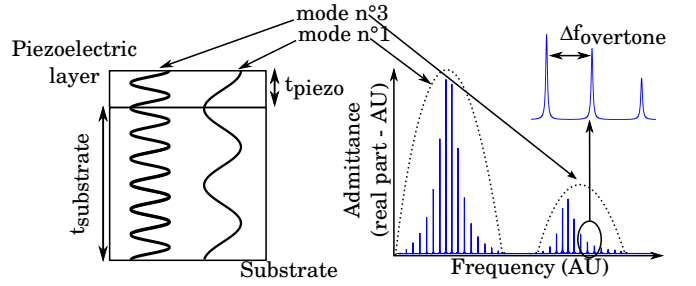


FIG. 1. Principle of the HBAR (left) and global view of the real part of the admittance (right).

The envelope of the HBAR response is defined by the piezoelectric layer thickness while the frequency span between each narrow resonance is defined by the substrate layer thickness. Considering first only the piezoelectric layer of thickness  $t_p$ , the resonance frequencies  $f_{mode}(n)$  are related to the acoustic velocity  $c$  by

$$f_{mode}(n) = n \times \frac{c}{2t_p} \quad (4)$$

at which the envelope of the admittance is maximum since the piezoelectric thin film pumps a maximum of energy in the substrate by inverse piezoelectric electromechanical conversion.

Once the acoustic energy has been coupled to the substrate of thickness  $t_s$ , the frequency spacing  $\Delta f_{overtone}$  between narrow resonances is given by

$$\Delta f_{overtone} \approx \frac{c}{2t_s} \quad (5)$$

This multitude of modes opens a unique perspective for exploiting the HBAR as gravimetric transducer: wideband acoustic spectroscopy of the mechanical properties of the adsorbed thin film. However, such an approach can only be exploited quantitatively if the gravimetric sensitivity of each mode is known.

Two HBAR geometries are considered. A  $3.8 \mu\text{m}$  thick AlN piezoelectric thin film deposited on a  $25.3 \mu\text{m}$ -thick SiO<sub>2</sub> substrate only confines longitudinal waves exhibiting wavelengths ranging from 2 to  $8 \mu\text{m}$  when operating

at frequencies in the 500 MHz to 5 GHz range. Since longitudinal waves are not appropriate for sensing in liquid media (acoustic radiative losses), the second geometry combines – following the IEEE 176-1987 (section 3.6) naming convention – a lithium niobate  $\text{LiNbO}_3$  YXl/163° thin film (selected for its high coupling characteristics) over a YXl/32° quartz substrate (selected for its low acoustic losses characteristics and low temperature sensitivity): the very different technological processes induce thicker layers of  $20 \mu\text{m}^{16}$  and  $450 \mu\text{m}$  respectively<sup>17,18</sup>. The latter device propagates pure shear waves and is hence compatible with the detection of compounds in liquid phase.

### III. MODELING

For modeling the HBAR resonator admittance and determining the gravimetric sensitivity of the various overtones as boundary conditions are varied, a one dimension modeling software is used based on Boundary Element Modeling (BEM)<sup>19,20</sup>. The free parameters tuned during the modeling process are the layer thicknesses and material properties, while the gravimetric sensitivity is extracted from the application of Eq. 1 when the resonance frequency is monitored as a function of adlayer geometrical properties and most significantly its thickness  $\Delta e$ .

#### A. Gravimetric sensitivity dependencies

The study first focuses on the impact of the side of the HBAR selected as the sensitive surface. Although a practical consideration naturally hints at using the side opposite to the piezoelectric layer coated with electrodes as the sensing area, the gravimetric sensitivity of both sides of the HBAR (the exposed area of the piezoelectric layer or the substrate) will exhibit different coupling with the adlayer and hence different gravimetric sensitivities (Fig. 2). Two adlayer mechanical properties are considered by selecting material constants of silica or copper. The gravimetric sensitivities are calculated by considering an adsorbed thickness of 5 nm to remain in a perturbative assumption.

Both adlayer characteristics yield similar gravimetric sensitivities, complying with the perturbation requirement of independence of the result with the thin additional film material properties. However, the evolution of  $S$  is radically different depending on which side of the HBAR is considered. In the first case in which the adlayer coats the substrate side, the gravimetric sensitivity decreases when the admittance is maximized and a tradeoff must be met between mode coupling and sensitivity: the gravimetric sensitivity is maximized at resonance frequencies below and above the piezoelectric thin film resonance frequency. The trend is opposite when coating the piezoelectric (top) side of the HBAR: in this

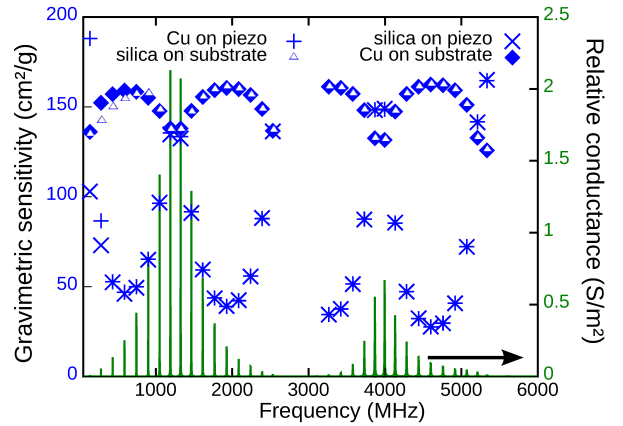


FIG. 2. Modeled HBAR admittance (solid line) and associated gravimetric sensitivity using two materials (copper and silica) on the top (piezoelectric layer) and bottom (substrate layer) sides of the HBAR.

case, both admittance and gravimetric sensitivity evolve similarly. The gravimetric sensitivities at the resonances of the piezoelectric thin film are the same whether the coating is deposited on the bottom or top sides.

While the gravimetric sensitivity remains constant within 10% when loading the substrate side, it varies significantly – in this case by a factor of 3 – when loading the piezoelectric layer side: hence, the probed modes must be carefully selected for maximizing both sensitivity and signal to noise ratio through efficient electromechanical coupling.

#### B. Thick film condition

In order to match experimental conditions, we shall from now on only consider an adlayer deposited on the substrate side, opposite to the electrodes polarizing the piezoelectric thin film. This strategy is selected so that packaging issues are only related to liquid confinement over the HBAR sensing surface and no electrical insulation or shielding issues arise when operating with compounds in liquid media.

Because on the wide range of operating frequencies, the perturbative assumption is hardly met at the higher frequency range, and based on the previous work presented by Mansfeld in<sup>21</sup> we now focus on modeling the behaviour of thick adsorbed films. “Thick” is defined as a film exhibiting significant departure from the behaviour predicted by Sauerbrey. Considering a thick film induces an uncertainty as to the definition of the initial condition when computing the sensitivity. On the one hand, the sensitivity is defined as an infinitesimal frequency variation due to an infinitesimal deposited mass: as such, the sensitivity is related to the derivate of the frequency versus adsorbed layer thickness. This case is closely related

to the one studied in<sup>21</sup> since a thick film acts as a gas absorbing layer and the sensitivity of the transducer coated with the thick film is considered. On the other hand, if the initial condition is considered to be the layer-free transducer, then the sensitivity is computed as the frequency variation due to a thick absorbed layer, no longer complying with the derivate approximation only valid for infinitesimal variations. The sensitivity computed by the latter approach is not only lower than the sensitivity derived from the derivate approach, but the thickness at which the sensitivity is maximized is not the same depending on the selected approach due to the curvature of the frequency v.s thickness curve, as shown in Fig. 3. Such conditions match our experimental assesment of the sensitivity by electro-depositing copper layers on the bare HBAR surface up to thicknesses matching the wavelength. In the following text, we consider the former approach as a thin film approach, even though we are considering a small increase of an already thick layer, while the latter will be called the thick film approach,

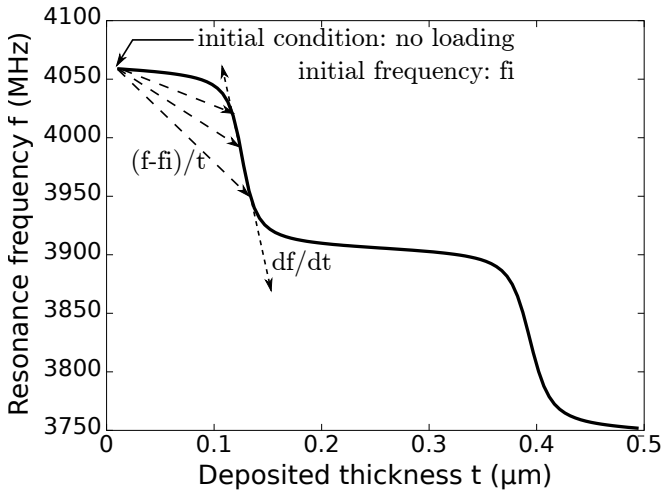


FIG. 3. Typical curve exhibiting the evolution of the resonance frequency of one mode of the HBAR as a function of absorbed layer thickness: the sharp rise in the frequency v.s thickness slope is observed for deposited thicknesses equal to multiples of the quarter wavelength. The frequency variation due to an absorbed layer thickness  $t$  depends on whether the initial condition is considered to be the bare transducer or the transducer already coated with a thick film. The latter approach always yields a larger estimate of the sensitivity than the former, as shown by the dotted lines representing the local slope of the frequency v.s thickness curve.

Departure from the perturbative assumption is considered by modeling an adlayer thickness of the same order than the wavelength. The results in the thick film approach, for two working frequencies, 1324 and 4000 MHz corresponding to wavelengths of 2.1 and 0.68  $\mu\text{m}$  respectively, are presented in Fig. 4.  $S$  is calculated for thicknesses of an adlayer, assumed to meet the material properties of copper, ranging from 50 nm to 2.5  $\mu\text{m}$ . Both overtones exhibit oscillating gravimetric sensitivities as a

function of adlayer thickness following the initial drop, with a period dependent on the overtone wavelength, yet the asymptotic sensitivity value remains the same at about 60  $\text{cm}^2/\text{g}$ .

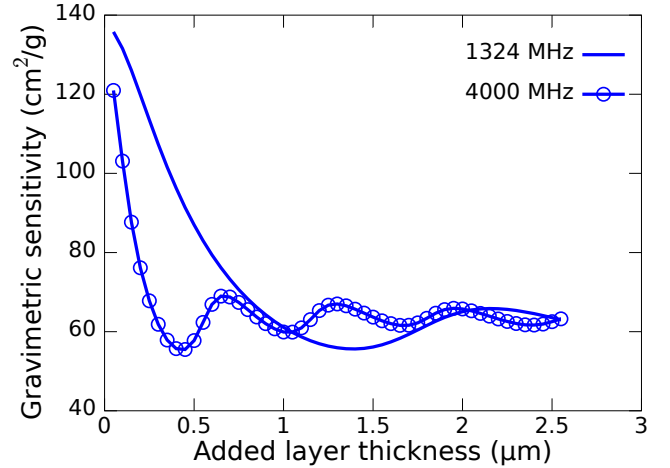


FIG. 4. Gravimetric sensitivity calculated as a function of the thickness of the copper adlayer for 1324 (solid line) and 4000 MHz (circles) resonance frequencies.

The same analysis in the thin film approach provides a clearer view of the resonant confinement of the acoustic energy in the thick absorbed film, as shown in Fig. 5. The frequency v.s thickness results are the same than those shown in Fig. 4 but here the initial state for computing the sensitivity value is selected as the infinitesimally thinner layer, hence compatible with the derivate of the frequency v.s thickness computation. Not only are the thicknesses at which sensitivity is maximum closely equal to multiples of the wavelength, but the actual sensitivity values remain close to the thin film value at odd multiples of the half wavelength – 120  $\text{cm}^2/\text{g}$  – as opposed to the thick film approach in which the sensitivity remained consistently lower than the perturbative layer sensitivity.

These results indicate that various overtones react differently to an adlayer of varying thickness due to the evolution of the energy distribution between the three layers – adlayer, piezoelectric thin film and substrate – in a coupled resonator context, making the wideband acoustic spectroscopy analysis non-trivial. An optimum operating frequency can be selected if the adlayer thickness is fixed and known in order to maximize  $S$ : such a conclusion was already reached in a previous analysis<sup>21</sup>. However, Mansfeld<sup>21</sup> determined theoretically and experimentally that the adlayer thickness maximizing  $S$  would be  $\lambda/4$ : this conclusion is not validated in the present case. To investigate the cause of the differences, several kinds of adsorbed material (Tab. I) used as perturbative layer are considered to assess the dependence of this conclusion with adlayer properties (Fig. 6).

The validity of the approach is assessed by first considering a silicon adlayer – the same material the HBAR is

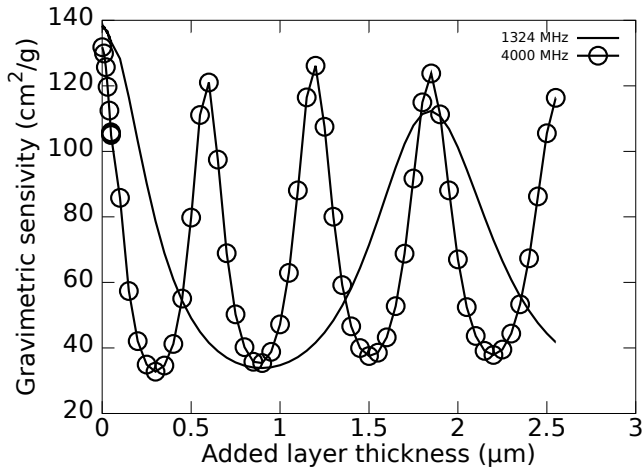


FIG. 5. Thin film analysis of the gravimetric sensitivity using the same simulation results than those exhibited in Fig. 4.

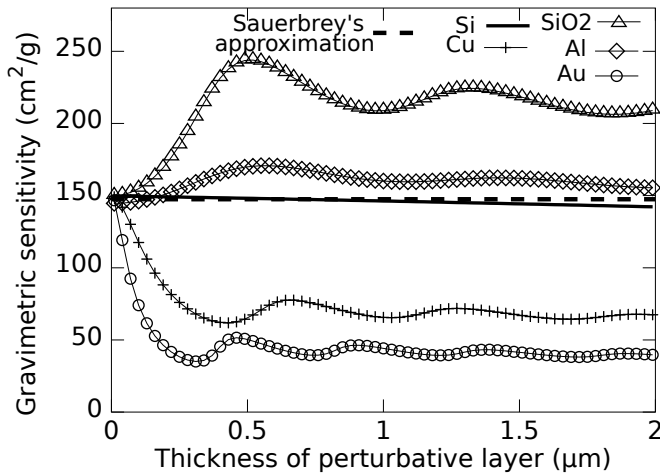


FIG. 6. Gravimetric sensitivity as a function of adlayer thickness, calculated for a working frequency of 4 GHz. Silica, aluminum, chromium, silicon and gold are considered as perturbative layer materials when computing the the gravimetric sensitivity. The dashed line corresponds to the gravimetric sensitivity calculated by Sauerbrey's approximation, considering a silicon resonator with a thickness of 29.1  $\mu\text{m}$ , equal to the global thickness of the simulated HBAR.

made off – and checking that the resulting sensitivity is indeed equal to the value predicted by the Sauerbrey perturbation theory (Fig. 6, dashed line and solid line) and independent of the adlayer thickness. For other adlayer materials (copper and gold) with an acoustic impedance higher than that of the silicon substrate,  $S$  decreases with increasing thickness as was previously observed in Fig. 4. For materials (silica and aluminum) with lower acoustic impedance than that of the substrate, the gravimetric sensitivity increases when the thickness increases.

These results demonstrate that the maximum of the gravimetric sensitivity depends on the relative acoustic

TABLE I. Acoustic impedances of the materials used for gravimetric sensitivity determination of a silicon HBAR.

| materials                 | $Z_{ac}$<br>(MRayl) | velocity<br>(m/s) |
|---------------------------|---------------------|-------------------|
| Silica ( $\text{SiO}_2$ ) | 13                  | 5740              |
| Aluminum (Al)             | 14                  | 5018              |
| <b>Silicon (Si)</b>       | <b>17</b>           | <b>7483</b>       |
| Copper (Cu)               | 24                  | 2728              |
| Gold (Au)                 | 29                  | 1480              |
| Aluminum nitride (AlN)    | 30                  | 11500             |
| YAG                       | 36                  | 7801              |

impedances and adlayer thickness to wavelength ratio. Furthermore, an increase of the gravimetric sensitivity can be obtained with an adsorbed material with acoustic impedance lower than that of the substrate as is classically known from the Love wave configuration: such an approach will be discussed in section V.

### C. Comparison with Mansfeld's theory

Although numerical constants are not provided in<sup>21</sup> for a direct comparison with these results, their use of YAG as a high acoustic impedance substrate<sup>22</sup>, exhibiting a high acoustic velocity, as the HBAR substrate, and the organic layer acting as the adlayer, hints at a case in which a low impedance coating is deposited over a high impedance substrate. Such a stack matches the qualitative behaviour identified by our numerical simulation. The quantitative assesment of the layer thickness maximizing the gravimetric sensitivity however requires an in-depth analysis of the sensitivity dependence with material properties. Such considerations are demonstrated in Fig. 7 which exhibits the acoustic wavelength (normalized to the layer thickness) at which the gravimetric sensitivity is maximized, as a function of the adlayer acoustic impedance. The gravimetric sensitivity is calculated using the thin film approach to be comparable with<sup>21</sup> in which the resonant frequency variation is recorded for an infinitesimal thickness variation of the adlayer due to gas adsorption. The results presented here consider an adlayer material with a constant Young's modulus (13 GPa) and various densities and Poisson coefficients. The elastic constants ( $C_{11}$ ,  $C_{12}$ ,  $C_{66}$ ) of the material are calculated for each density and Poisson coefficient values. Maximizing the sensitivity for a  $\lambda/4$  thickness of the adlayer is consistent in some cases which present a low Poisson coefficient (less than 0.2) and different acoustic impedance of the adsorbed material. The BEM approach used here takes in account all the elastic constants of the materials and so exhibits more rigorous results than the analytical approach.

The gravimetric sensitivity dependence with overtone number (and hence wavelength) and material property of the adlayer has been investigated through simulation, demonstrating a non-trivial link between these relations.

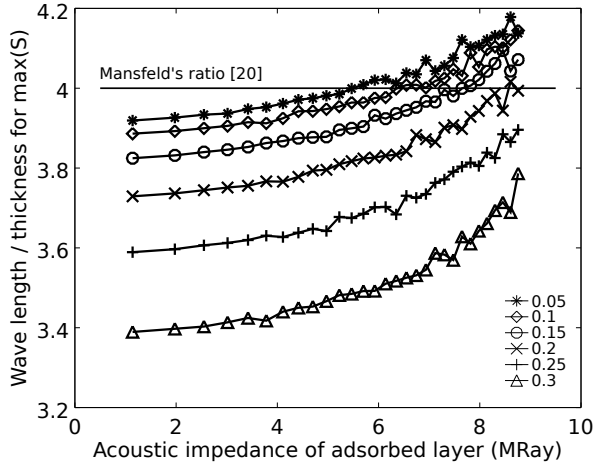


FIG. 7. Ratio of the acoustic wavelength in the adlayer to the adlayer thickness maximizing the gravimetric sensitivity. The solid line indicates the value cited by Mansfeld when considering an organic layer over a YAG substrate, the marked lines are the result of our simulation for varying acoustic impedance adlayers and using different poisson coefficients over a silicon HBAR.

A low impedance adlayer is predicted to magnify the gravimetric sensitivity. Moreover, results cited earlier in the literature could be modeled in detail during these investigations, whose results will now be confronted to experimental results.

#### IV. EXPERIMENTAL RESULTS

Experimental assessment of the gravimetric sensitivity of HBARs is performed in two distinct steps: on the one hand the irreversible deposition of thin copper films in a cleanroom environment by sputtering, and on the other hand the reversible electrodeposition of copper in a wet environment. All depositions are performed on the substrate side of the HBAR, opposite to the electrodes deposited on the piezoelectric thin film. The admittance of the HBAR is monitored by a network analyzer, either after each deposition step in the case of the sputtering, or continuously during the electrochemical oxydation and reduction cycles. Since part of these experiments will be performed in a wet environment, only the lithium niobate over quartz HBAR propagating pure shear waves is considered.

The HBAR is characterized at four different frequency ranges (280-310 ; 410-440 ; 670-700 ; 800-830 MHz). Each frequency range presents about seven resonances. As shown on table II, the gravimetric sensitivity for each resonance is calculated by considering the initial resonant frequency as the resonance frequency obtained with the previous adlayer thickness (thin film approach). The acoustic wavelengths for each frequency range are close,

so only the mean value of the gravimetric sensitivities is presented and all thicknesses are normalized to the acoustic wavelength in the adlayer (Fig. 8).

TABLE II. Experimental gravimetric sensitivity mean value calculated for each frequency range and for each deposited copper thickness.

| Deposited thickness (nm) | Mean of gravimetric sensitivity ( $\text{cm}^2/\text{g}$ ) |             |             |             |
|--------------------------|--|-------------|-------------|-------------|
|                          | 280-310 MHz  | 410-440 MHz | 670-700 MHz | 800-830 MHz |
| 196                      | 10.5   | 7.2         | 4.5         | 5.1         |
| 381                      | 7.7  | 5.5         | 3.5         | 3.7         |
| 541                      | 7.0  | 5.0         | 3.3         | 3.4         |
| 726                      | 6.3  | 4.5         | 3.1         | 3.4         |
| 891                      | 5.8  | 4.2         | 3.2         | 3.9         |
| 1099                     | 5.2  | 3.8         | 3.5         | 4.6         |
| 1299                     | 4.8  | 3.6         | 4.2         | 4.8         |
| 1514                     | 4.4  | 3.4         | 4.6         | 4.5         |

Both experimental and modeled (Fig. 8) dependences of the gravimetric sensitivity with the adlayer thickness hint at a starting value of about  $10 \text{ cm}^2/\text{g}$  and a secondary maximum. **The discrepancy between the modeled and experimental results, yielding different adlayer thicknesses maximizing the sensitivity, is attributed to the use of bulk material constants which might not appropriately represent the thin copper film properties.**

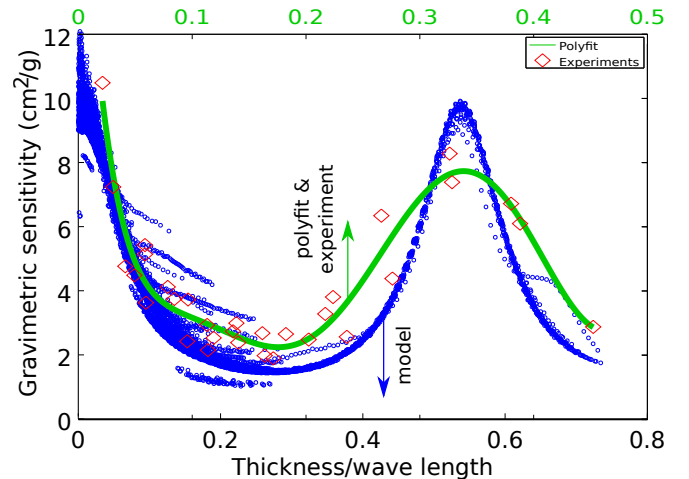


FIG. 8. Mean value of the measured gravimetric sensitivity for each frequency range (diamonds) as a function of the deposited thickness divided by the acoustic wavelength, and polynomial fit (solid line) as a guide for the eye. Circles: gravimetric sensitivity estimates resulting from modeling the lithium niobate over quartz HBAR stack considered in the experimental section: the different curves are associated with different overtones. Notice that the two charts do not share the same abscissa: the experimental data abscissa is given on top, the model abscissa is given on the bottom. The gravimetric sensitivity (ordinate) is properly modeled and shared by the two charts.

An alternative to cleanroom sputtering of copper is the use of electrochemical deposition on the sensing surface of an HBAR. This approach, already used to charac-

terize the gravimetric sensitivity of QCM<sup>23</sup>, SAW<sup>24</sup> and HBAR<sup>25</sup> devices, is attractive because it is reversible (allowing for multiple cycles for assessing the reproducibility of the result) and operates in liquid phase, hence being more representative of the behaviour of the sensor used for detecting compounds in aqueous solutions (e.g. biosensing). This method is only usable with devices propagating pure shear waves due to viscoelastic coupling of the propagating longitudinal waves. The chemical reaction is driven by a custom-made potentiostat included in the embedded electronics<sup>15</sup> designed to probe simultaneously multiple overtones of the HBAR. This electronics provides a measurement rate large enough to be compatible with the reaction kinetics.

The gravimetric sensitivity of an overtone at 327 MHz of the lithium niobate/quartz HBAR is investigated: electrochemical deposition provides an independent estimate of the adlayer mass  $m_{Cu}$  through Eq. 1, assuming a 100% yield, by considering the number of electrons involved in the reduction process as the integral of the current  $i(t)$  flowing through the working electrode

$$m_{Cu} = \frac{M_{Cu} \times \int i(t) dt}{N_A \times e \times n_e} \quad (6)$$

where  $M_{Cu}$  is the molar weight ( $g/mol$ ) of the adlayer,  $\int i(t) dt$  the number of charges transferred during electro-deposition, considering that the charge of one mole of electrons ( $N_A$ ) is 96440 C, and  $n_e$  the number of electrons transferred during the redox reaction (Eq. 7)



Fig. 9 exhibits the gravimetric sensitivity measured using the electro-deposition approach and the modeling of the used HBAR, both considered at the same working frequency. This working frequency is fixed and used as the initial resonant frequency (thick film approach). The thin film approach for calculating the gravimetric sensitivity could not be used in this case due the experimental set up which does not allow to have the resonant frequency between each adlayer thickness. Knowing the area  $A$  of the sensing side of the HBAR over which the electrochemical reaction occurs, Eq. 1 and 6 allow for estimating the deposited thickness. Hence, the gravimetric sensitivity is plotted as a function of the deposited thickness. Experiment matches the modeled sensitivities for adlayer thicknesses above 1.2  $\mu m$ . Below this value, the calculated sensitivity is 3 to 6 times higher than the model results. The main cause of divergence of the two curves for thin adlayers is attributed to the inhomogeneous deposition which starts at the center of the HBAR sensing area. In such cases, the estimated adlayer thickness  $\Delta e = m_{Cu}/A$  is under-estimated since  $A$  is overestimated when using the geometrical area, and the experimental sensitivity is hence over-estimated.

Based on these considerations, the HBAR geometries considered so far exhibit sensitivities consistent with those of bulk QCMs and hence 10 to 20 times lower than

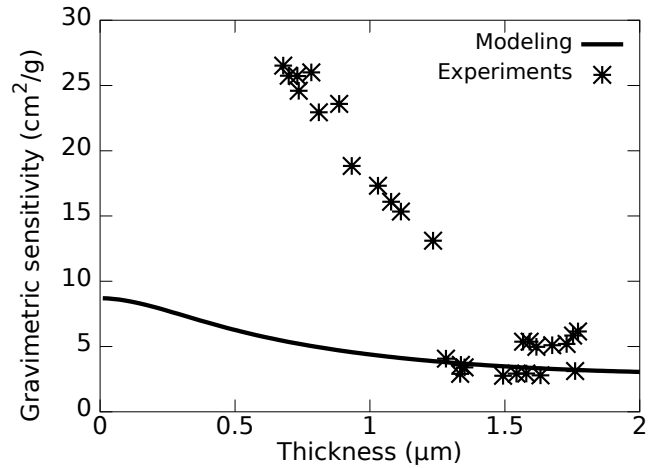


FIG. 9. Gravimetric sensitivity measured (stars) and modeled (solid line) for a lithium niobate over quartz HBAR operating at 327 MHz, as a function of the electrochemically deposited layer thickness.

SAW devices operating in the hundreds of MHz range. However, the low-acoustic impedance adlayer has been shown to increase the gravimetric sensitivity, so we consider whether an additional stack of material over the HBAR might bring some gravimetric sensitivity improvement, aiming at the hundreds of  $cm^2/g$  range classically found for Love-mode SAW devices<sup>24</sup>.

## V. GRAVIMETRIC SENSITIVITY IMPROVEMENT

Two ways to improve the gravimetric sensitivity have been theoretically explored. Since the Sauerbrey gravimetric sensitivity depends on the working frequency which depends on the thickness of the QCM, reducing the overall sensor thickness will be considered. Based on this idea, the gravimetric sensitivity is calculated for lithium niobate over quartz HBARS when varying the substrate thickness from 56.25 to 450  $\mu m$  (Tab. III).

TABLE III. Calculated gravimetric sensitivity for different thicknesses of quartz substrate. Frequency ranges and the number of probed modes are also presented.

| Frequency range (MHz)                    | 50 - 150 |     |       |       | 300 - 550 |     |       |       |
|--|----------|-----|-------|-------|-----------|-----|-------|-------|
| Quartz thickness ( $\mu m$ )             | 450      | 225 | 112.5 | 56.25 | 450       | 225 | 112.5 | 56.25 |
| number of probed modes                   | 53       | 28  | 14    | 7     | 51        | 26  | 13    | 8     |
| avg. sensitivity ( $cm^2/g$ )            | 9        | 18  | 37    | 80    | 8         | 16  | 31    | 59    |
| theoretical sens. (Sauerbrey. $cm^2/g$ ) | 8        | 17  | 34    | 67    | 8         | 17  | 33    | 67    |

Although this approach trivially scales the sensitivity as the substrate thinning ratio, closely matching the

Sauerbrey equation prediction, the transducer ruggedness is impacted and the solution is not satisfactory in reaching disadvantages of FBARs.

A second investigated way of improvement is adding a well-chosen material on the sensitive surface of the HBAR. The gravimetric sensitivity depends on the impedance of the deposited materials (Fig. 6). Following a strategy proven in the case of the Love-mode SAW transducer, an additional layer is designed to confine the acoustic wave near the sensing surface to improve the gravimetric sensitivity. The efficiency of this approach is assessed by modeling the sensitivity of an AlN over silicon HBAR, coated with an additional layer of silicon oxide. In this calculation, the gravimetric sensitivity is calculated by considering a 5 nm-thick copper adlayer on the silicon oxide (Fig. 10).

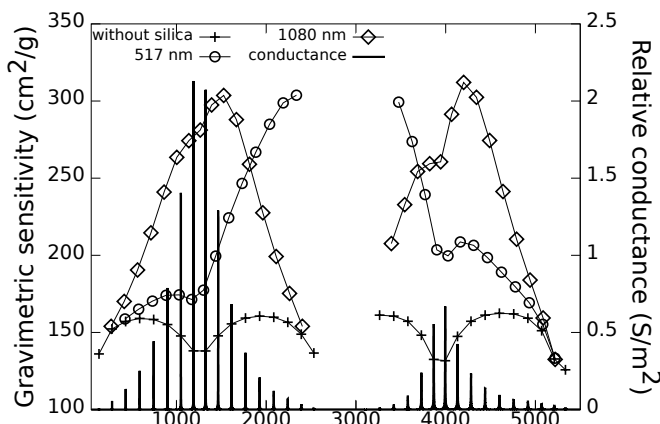


FIG. 10. Gravimetric sensitivity calculated for an AlN over Si HBAR with (lines with markers) and without (solid line) silicon oxide layer.

Different thicknesses of the silicon dioxide acoustic field confinement layer are considered (Fig. 10): the affected overtone varies as a function of the silicon dioxide layer thickness, but in all cases a dramatic sensitivity enhancement is observed, with a doubling of the sensitivity with respect to the bare device.

## VI. CONCLUSIONS

The gravimetric sensitivity of composite HBAR resonators has been studied to determine their potential as direct detection sensors. Two architectures, aluminum nitride over silicon and lithium niobate over quartz, are considered as complementary since the former exhibits high sensitivity – of the same order of magnitude as those found for 125 MHz Love mode SAW devices – but propagates longitudinal waves incompatible with sensing compounds in liquid phase, while the latter propagates pure shear waves yet only exhibits sensitivity with val-

ues around those exhibits by radiofrequency bulk acoustic resonators – typically 10 times lower than the Love-mode value. The multimode spectral characteristics of these transducers is considered best suited for wideband acoustic spectroscopy of adsorbed layers. However, the complex dependence of the gravimetric sensitivity of the various overtones yields non-trivial analysis considerations requiring accurate acoustic behaviour modeling of the coupled acoustic fields in the various layers. The poor gravimetric sensitivity of the bare device is theoretically improved by adding a low-acoustic impedance layer on the sensing area following a strategy reminiscent of the Love mode guided SAW device. Working on the electrode-free side of the HBAR solves the classical packaging issue of SAW devices since no structure needs to be located on the acoustic path while electrodes are prevented from being in contact with the medium containing the analyte being investigated.

## ACKNOWLEDGEMENTS

This work was supported by the French RENATECH network and its FEMTO-ST technological facility. Part of this work was funded by the French DGA through the ROHLEX grant and a Defense PhD funding, as well as by the European LOVEFOOD project (FP7-ICT-2011.3.2 grant).

- <sup>1</sup>E. Gizeli and C. R. Lowe, *Biomolecular sensors*. CRC Press, 2004.
- <sup>2</sup>D. Thévenot, K. Toth, R. Durst, and G. Wilson, “Electrochemical biosensors recommended definitions and classification,” *Biosensors and Bioelectronics*, vol. 16, no. 1, pp. 121–131, 2001.
- <sup>3</sup>J. Janata, *Principles of chemical sensors*. Springer, 2009.
- <sup>4</sup>J. Homola, S. S.Y., and G. Gauglitz, “Surface plasmon resonance sensors: review,” *Sensors and Actuators B: Chemical*, vol. 54, no. 1, pp. 3–15, 1999.
- <sup>5</sup>M. Taulés and J. Comas, “Overview of molecular interactions using Biacore,” *Capítol del llibre: Handbook of instrumental techniques for materials, chemical and biosciences research, Centres Científics i Tecnològics. Universitat de Barcelona, Barcelona, 2012. Part III. Biosciences technologies (BT), BT. 10, 10 p.*, 2012.
- <sup>6</sup>X.-L. Su and Y. Li, “A QCM immunosensor for salmonella detection with simultaneous measurements of resonant frequency and motional resistance,” *Biosensors and Bioelectronics*, vol. 21, no. 6, pp. 840–848, 2005.
- <sup>7</sup>P. Si, J. Mortensen, A. Komolov, J. Denborg, and P. J. Møller, “Polymer coated quartz crystal microbalance sensors for detection of volatile organic compounds in gas mixtures,” *Analytica chimica acta*, vol. 597, no. 2, pp. 223–230, 2007.
- <sup>8</sup>N. Moll, E. Pascal, D. H. Dinh, J.-P. Pillot, B. Bennetau, D. Rebière, D. Moynet, Y. Mas, D. Mossalayi, J. Pistré *et al.*, “A love wave immunosensor for whole *e. coli* bacteria detection using an innovative two-step immobilisation approach,” *Biosensors and Bioelectronics*, vol. 22, no. 9, pp. 2145–2150, 2007.
- <sup>9</sup>O. Tamarin, C. Déjous, D. Rebière, J. Pistré, S. Comeau, D. Moynet, and J. Bezian, “Study of acoustic love wave devices for real time bacteriophage detection,” *Sensors and Actuators B: Chemical*, vol. 91, no. 1, pp. 275–284, 2003.
- <sup>10</sup>T. Abe and Y. Itasaka, “A fabrication method of high-Q quartz crystal resonator using double-layered etching mask for DRIE,” *Sensors and Actuators A: Physical*, vol. 188, no. 1, pp. 503–506, 2012.



- <sup>11</sup>“Official website xeco,” <http://www.xeco.net>.
- <sup>12</sup>M. Nirschl, A. Blüher, C. Erler, B. Katzschner, I. Vikholm-Lundin, S. Auer, J. Vörös, W. Pompe, M. Schreiter, and M. Mertig, “Film bulk acoustic resonators for DNA and protein detection and investigation of in vitro bacterial S-layer formation,” *Sensors and Actuators A: Physical*, vol. 156, no. 1, pp. 180–184, 2009.
- <sup>13</sup>W. Xu, X. Zhang, S. Choi, and J. Chae, “A high-quality-factor film bulk acoustic resonator in liquid for biosensing applications,” *Microelectromechanical Systems, Journal of*, vol. 20, no. 1, pp. 213–220, 2011.
- <sup>14</sup>G. Sauerbrey, “Verwendung von Schwingquarzen zur Wägung dünner Schichten und zur Mikrowägung,” *Zeitschrift für Physik A Hadrons and Nuclei*, vol. 155, no. 2, pp. 206–222, 1959.
- <sup>15</sup>D. Rabus, J.-M. Friedt, S. Ballandras, G. Martin, E. Carry, and V. Blondeau-Patissier, “High-sensitivity open-loop electronics for gravimetric acoustic-wave-based sensors,” *IEEE Transactions on Ultrasonics, Ferroelectrics, and Frequency Control*, vol. 60, no. 6, p. 1219, 2013.
- <sup>16</sup>J. Masson, G. Martin, R. Boudot, Y. Gruson, S. Ballandras, A. Artieda, P. Muralt, B. Belgacem, and L. Chomeloux, “On the dispersive behaviour of aln/si high overtone bulk acoustic resonators,” in *Frequency Control Symposium, 2007 Joint with the 21st European Frequency and Time Forum. IEEE International*, IEEE, 2007, pp. 741–744.
- <sup>17</sup>S. Ballandras, T. Baron, E. Lebrasseur, G. Martin, S. Alzuaga, J.-M. Friedt, J. Poncot, and C. Guichard, “High overtone bulk acoustic resonators built on single crystal stacks for sensors applications,” in *Sensors, 2011 IEEE*. IEEE, 2011, pp. 516–519.
- <sup>18</sup>T. Baron, G. Martin, E. Lebrasseur, B. François, S. Ballandras, P.-P. Lasagne, A. Reinhardt, L. Chomeloux, J.-M. Lesage, and D. Gachon, “RF oscillators stabilized by temperature compensated HBARs based on linbo<sub>3</sub>/quartz combination,” in *Frequency Control and the European Frequency and Time Forum (FCS), 2011 Joint Conference of the IEEE International*. IEEE, 2011, pp. 1–4.
- <sup>19</sup>A. Reinhardt, T. Pastureaud, S. Ballandras, and V. Laude, “Scattering matrix method for modeling acoustic waves in piezoelectric, fluid, and metallic multilayers,” *Journal of applied physics*, vol. 94, no. 10, pp. 6923–6931, 2003.
- <sup>20</sup>S. Ballandras, M. Wilm, W. Daniau, A. Reinhardt, V. Laude, and R. Armati, “Periodic finite element/boundary element modeling of capacitive micromachined ultrasonic transducers,” *Journal of applied physics*, vol. 97, no. 3, pp. 034 901–034 901, 2005.
- <sup>21</sup>G. Mansfeld, “Theory of high overtone bulk acoustic wave resonator as a gas sensor,” in *Microwaves, Radar and Wireless Communications. 2000. MIKON-2000. 13th International Conference on*. IEEE, 2000, pp. 469–472.
- <sup>22</sup>L. Mezeix and D. J. Green, “Comparison of the mechanical properties of single crystal and polycrystalline yttrium aluminum garnet,” *International journal of applied ceramic technology*, vol. 3, no. 2, pp. 166–176, 2006.
- <sup>23</sup>J.-M. Friedt, K.-H. Choi, F. Frederix, and A. Campitelli, “Simultaneous AFM and QCM measurements methodology validation using electrodeposition,” *Journal of The Electrochemical Society*, vol. 150, no. 10, pp. H229–H234, 2003.
- <sup>24</sup>J.-M. Friedt, L. Francis, K.-H. Choi, and A. Campitelli, “Combined atomic force microscope and acoustic wave devices: Application to electrodeposition,” *J. Vac. Sci. Tech. A*, vol. 21, no. 4, p. 1500, July-Aug. 2003.
- <sup>25</sup>D. Rabus, G. Martin, E. Carry, and S. Ballandras, “Eight channel embedded electronic open loop interrogation for multi sensor measurement,” in *European Frequency and Time Forum (EFTF), 2012*. IEEE, 2012, pp. 436–442.